



Providing Choice & Value

Generic CT and MRI Contrast Agents



FRESENIUS
KABI

CONTACT REP

AJNR

**Scan-Rescan Variation of Measures Derived from
Brain Magnetization Transfer Ratio Histograms
Obtained in Healthy Volunteers by Use of a
Semi-interleaved Magnetization Transfer
Sequence**

Matilde Inglese, Mark A. Horsfield and Massimo Filippi

This information is current as
of July 19, 2025.

AJNR Am J Neuroradiol 2001, 22 (4) 681-684

<http://www.ajnr.org/content/22/4/681>

Scan-Rescan Variation of Measures Derived from Brain Magnetization Transfer Ratio Histograms Obtained in Healthy Volunteers by Use of a Semi-interleaved Magnetization Transfer Sequence

Matilde Inglese, Mark A. Horsfield, and Massimo Filippi

Summary: A novel semiinterleaved gradient-echo (GE) sequence for quantitative measurement of magnetization transfer ratio (MTR) is described. With this sequence, several lines of k-space are collected for the non-MT image then several lines are collected for the MT image, thus building up the entire k-space in distinct acquisition blocks, with a good trade-off between motion-induced misregistration and degree of MT effect. The scan-rescan coefficients of variation for several MTR histogram-derived measures from 10 healthy volunteers scanned serially with this semiinterleaved sequence proved to be lower than those achieved using a conventional GE sequence. This sequence may be useful in a clinical environment to measure MTR changes over time more reliably than when acquiring the non-MT and MT images sequentially, which inevitably are affected by patient motion.

Magnetization transfer ratio (MTR) histogram analysis is increasingly being used to assess brain disorders in numerous neurologic conditions, including multiple sclerosis (MS) (1). Animal (2) and postmortem human (3) studies have shown that brain areas with decreased MTR correspond to areas in which severe demyelination and axonal loss have occurred. The advantage of histogram analysis over more conventional region-of-interest analysis is that it provides quantitative indexes that reflect the overall extent of brain disease (4). This is particularly important in diseases, such as MS, with widespread, multifocal lesions of different sizes and heterogeneous intrinsic abnormalities, which may go undetected on conventional MR imaging sequences (5).

Quantities derived from MTR histograms are promising as objective and accurate measures for

monitoring treatment efficacy in MS. In this scenario, it is necessary to develop and use MR techniques with low intrinsic variability so as to increase the chances of detecting relatively small treatment effects. In most implementations of a quantitative MTR sequence, the two images (with and without MT saturation pulses) are collected sequentially, leading to the possibility of misregistration caused by patient movement, and consequent errors in the calculated MTR, particularly around the borders of imaging features. One way to overcome this liability is to collect lines of k-space alternately, first from the non-MT image and then from the MT image (6). However, saturation of the macromolecular magnetization may take several seconds, and magnetization saturation must first be built up for the MT image and then be allowed to decay for the non-MT image, leading to extended imaging times.

An intermediate approach, explored in the present study, is to collect several lines of k-space for the non-MT image, then several lines for the MT image, and thus build up the entire k-space in distinct acquisition blocks. The rationale for this approach is that the time spent acquiring data with the macromolecular magnetization saturation not in steady-state is relatively small, and so the MT values should be close to those for sequential acquisition of the non-MT and MT images. However, since the k-space data are acquired in a semiinterleaved fashion, the possibility of incurring misregistration artifacts is also greatly reduced. We refer to the pulse sequence that implements this approach as the semiinterleaved sequence, and we report the scan-rescan variability in the assessment of several MTR histogram-derived measurements obtained serially from 10 healthy volunteers who were scanned using this sequence.

Methods

Subjects

Ten healthy volunteers (five women and five men; mean age, 31 years, range 27–34 years) entered the study after providing informed consent. Approval from the local ethical committee was also obtained before study initiation. None of the partic-

Address reprint requests to Dr. Massimo Filippi, Neuroimaging Research Unit, Department of Neuroscience, Scientific Institute Ospedale San Raffaele, via Olgettina 60, 20132 Milan, Italy.

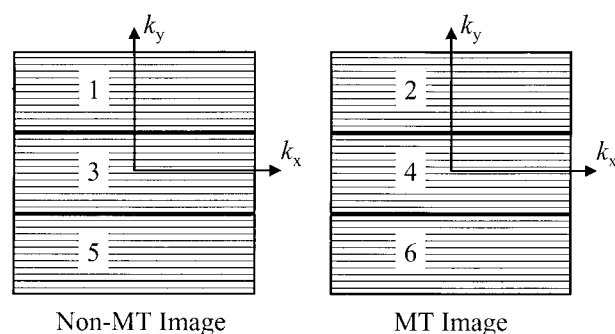


FIG 1. Data collection scheme for the semiinterleaved MT sequence. For each image, k-space data are collected in three blocks. The first one third of the non-MT image (block labeled 1) is followed by the first one third of the MT image (block labeled 2). This is followed by acquisition of the second and third blocks of the two images (labeled 3 through 6) in this semiinterleaved fashion. For the first few lines of blocks 2 through 6, the macromolecular magnetization saturation is not in a steady state, leading to slightly lower MT values than for sequential acquisition, but the likelihood of misregistration between the non-MT and MT images is considerably reduced.

ipants had a history of neurologic diseases or neurologic signs at clinical examination.

Image Acquisition

MR images of the brain were obtained using a 1.5-T unit with a maximum available gradient strength of 21 mTm^{-1} and a maximum slew rate of $167 \text{ Tm}^{-1}\text{s}^{-1}$, from each participant on two occasions separated by $28 (\pm 5)$ days. A birdcage head coil with a diameter of approximately 300 mm was used for both radio frequency (RF) transmission and signal reception. On each imaging occasion, we obtained the following sequences: 1) a dual-echo spin-echo sequence (2400/30,80/1 [TR/TE/excitations]) with 24 contiguous, interleaved, 5-mm-thick axial sections, a 256×256 matrix, and a 250-mm field of view; 2) a conventional gradient-echo (GE) sequence (600/12/2, α , 20°) with 20 contiguous, interleaved, 5-mm-thick axial sections, a 256×256 matrix, and a 250-mm field of view; and 3) the new semiinterleaved GE sequence with the same acquisition parameters as for sequence 2 (Fig 1). Sequence 2 was performed twice: first without then with an MT saturation pulse. The RF saturation pulse was centered 1.5 kHz below the water frequency, with a gaussian envelope of a duration of 7.68 milliseconds, a bandwidth of 250 Hz, and a flip angle of 500° . The same saturation pulse was used for sequence 3 (the semiinterleaved sequence), in which the two images with and without the MT saturation pulses were collected in a semiinterleaved fashion. For each image, the coverage of k-space was split into three parts, in which one third of the k-space were lines collected without saturation pulses and then one third were collected with saturation pulses. This was then repeated for the second and third portions of k-space. The aim of this design was to reduce misregistration of the two images that can arise with sequential collection of the image data, but to maintain an acceptably short scan time by collecting k-space data in blocks. If MT/non-MT images are collected in a truly interleaved fashion, then a long TR must be allowed for the buildup and decay of magnetization saturation between the separate interleaves (6). Magnetization saturation reaches a steady state after a time equal to several T1 periods (7), and with the semiinterleaved approach and a TR of 600, this should be the case after six to 10 lines of k-space, resulting in image contrast produced by MT effects similar to that seen in a sequentially acquired pair of images.

The choice of three acquisition blocks for the semiinterleaved sequence was governed by three factors. First, because we

wanted to traverse the central portion of k-space without interruption, we changed from data collection without saturation pulses to data collection with the saturation pulses, which necessitated an odd number of acquisition blocks. Second, we wanted the time to acquire any one block to be considerably longer than the T1 of any of the tissues of interest in order to have a minimal impact on MTR values. The number of acquisition blocks represents a compromise between robustness in the face of patient movement and MT effect; we estimated that with acquisition split into more than nine blocks, the calculated MTR values would begin to show marked reductions as more of the lines of k-space were acquired with the macromolecular magnetization not in steady state. Finally, and crucially for this study, the limitations of our scanner software did not allow more than three blocks to be programmed. Acquisition time for sequences 2 and 3 were each 10 minutes 14 seconds.

Image Analysis

The conventional and the semiinterleaved GE images were transferred to a workstation and quantitative MTR images were derived pixel by pixel, using software developed in house, according to the following expression: $\text{MTR} = (M_0 - M_S)/M_0 \times 100$, in which M_0 is the signal intensity for a given pixel without the saturation pulses and M_S is the signal intensity for the same pixel when the saturation pulses are applied. Signal intensities in the calculated images represent the MTR values. For the conventional GE sequence, images obtained before and after the application of the MT pulse were coregistered using a surface-matching technique based on mutual information (8).

Histograms of the MTR images were then created. First, for each of the two MTR images, a single observer segmented the brain from the surrounding tissue by using a semiautomated segmentation technique based on local thresholding (9) and then followed the postprocessing technique described in detail elsewhere (10) to obtain the brain MTR histograms. To correct for the between-subject differences in brain volume, each histogram was normalized by dividing the height of each histogram bin by the total number of pixels included (4). For each histogram, the following measures were derived: the average brain MTR, the relative peak height (ie, the proportion of pixels at the most common MTR value), and the peak position (ie, the most common MTR). For each of these, the scan-rescan variability was calculated using the coefficient of variation (COV). The COV was defined as the SD of a random variable divided by its mean value. The standard errors (SE) of the COV were estimated using the bootstrap resampling technique (11).

Results

No abnormalities were seen on the dual-echo images of these healthy subjects. The mean values and SD of the MTR histogram-derived measurements averaged over the two occasions for the 10 subjects and the two GE sequences are reported in Table 1. The corresponding mean values and SE for scan-rescan COVs are reported in Table 2.

Discussion

MTR histogram analysis is an intriguing approach to monitoring the effects of experimental treatment on the overall brain lesion burden in multifocal neurologic conditions, such as MS. However, before using such an approach in the context of clinical trials, it is necessary to demonstrate that the technique is reproducible. Reproducibility of

TABLE 1: MTR histogram-derived measurements obtained from 10 healthy volunteers scanned on two separate occasions using conventional and semiinterleaved gradient-echo sequences

Sequence	Average MTR (SD) [%]	Mean Peak Height (SD) [%]	Mean Peak Position (SD) [%]
Conventional	39.0 (0.8)	114.2 (10.2)	35.1 (1.3)
Semiinterleaved	37.6 (0.7)	125.5 (13.8)	31.8 (1.4)

Note.—MTR indicates magnetization transfer ratio.

TABLE 2: Scan-rescan COV (%) for the MTR histogram-derived measurements obtained from 10 healthy volunteers scanned on two separate occasions using conventional and semiinterleaved gradient-echo sequences

Sequence	Average MTR (SE)	Mean Peak Height (SE)	Mean Peak Position (SE)
Conventional	1.8 (0.2)	7.9 (1.9)	3.8 (0.4)
Semiinterleaved	1.6 (0.4)	7.8 (2.3)	3.1 (0.6)

Note.—COV indicates coefficient of variation; MTR, magnetization transfer ratio.

MR measurements is influenced by several factors, including the use of different scanners, sequences, and observers, as well as by the day-to-day variability of the scanner and the image evaluator (ie, the so-called scan-rescan variability). Of these factors, scan-rescan variability is by far the most important, since the same scanner, sequence, and observer can be used to collect and analyze sequential MR data from each patient. In the case of MT imaging, one variable that can impinge on reproducibility is patient movement, which may occur between the acquisition of the two images (with and without the saturation pulse) necessary to obtain MTR maps. Even very small shifts may be enough to render invalid the calculated MTR values in regions of the brain in which image intensity is varying rapidly with position (eg, in small lesions). This would affect both global and regional analysis of MTR values. Since image acquisition usually takes several minutes, such movement is not at all unlikely, particularly in the case of severely disabled, uncooperative, or cognitively impaired patients.

This problem with conventional MT sequences can be overcome by interleaving the MT and non-MT acquisitions, but with the penalty of longer scan times (6). In this study, we investigated a new semiinterleaved sequence for quantitative measurement of MTR with a good trade-off between motion-induced misregistration and image acquisition time. For non-MT and MT images acquired sequentially and not coregistered, it was shown in a previous study of reproducibility (12) that the scan-rescan COV of average MTR was 2.2%. In the current study, we found that the COV of average MTR was 1.6% when using the new semiinterleaved sequence (ie, it was reduced by about 30%), while other measures remained virtually unchanged relative to those of the previous study (12). Even

though in the present study coregistration was used for the sequentially acquired images, the scan-rescan COVs were all slightly better when the new semiinterleaved sequence was used. Elimination of the need for complex and time-consuming image registration is an obvious advantage for the production of quantitative MTR images, particularly when this is implemented, for example, directly on the scanner console.

Acquisition time for the semiinterleaved sequence was 10 minutes 14 seconds, the same as for the conventional GE MT sequence, although this could be reduced to 7 minutes 40 seconds, without changing the in-plane resolution, by using a 3/4 field of view and a 192×256 matrix. A truly interleaved sequence with the same number of slices, excitations, and in-plane resolution would have taken about 64 minutes by our estimate. Thus, previous work with interleaved acquisition has limited the number of slices and the image matrix to maintain an acceptable imaging time of 10 minutes (6). However, limited brain coverage and poor in-plane resolution may not be desirable when studying MS, which is a multifocal disease involving the entire brain, sometimes with very small lesions (13).

The semiinterleaved approach will inevitably lead to slightly reduced MTR values, as indicated by the evidence in Table 1, because some of the lines of k-space in each block are acquired before a steady state of magnetization saturation is reached, with the degree of reduction depending on the number of blocks into which the acquisition is segmented. This would not necessarily be a disadvantage unless comparison of MTR values with another sequence was necessary. However, if high MTR values were important, then this could be improved by adding a few dummy lines to the start of each acquisition block, in which the pulse sequence applies the RF and gradient pulses as usual but no data are collected, to force the magnetization into steady state before data collection begins. Nevertheless, the MTR values are higher than those reported with the fully interleaved approach (6), perhaps because of a compromise in the time allowed for macromolecular magnetization saturation and relaxation. Finally, the semiinterleaved approach is amenable to incorporation into a 3D-GE acquisition scheme with the acquisition segmented into blocks in the second phase-encoded direction, which would enable production of accurately registered high-resolution MTR maps.

Acknowledgments

We are grateful to M. P. Sormani for her help in performing the COV calculations, and to personnel at Siemens Medical, both in Germany and in the UK, for assistance with pulse sequence implementation.

References

1. Grossman RI. Magnetization transfer in multiple sclerosis. *Ann Neurol* 1994;36:S97-S99

2. Brochet B, Dousset V. **Pathological correlates of magnetization transfer imaging abnormalities in animal models and humans with multiple sclerosis.** *Neurology* 1999;53(Suppl 3):S12-S17
3. van Waesberghe JHTM, Kamphorst W, De Groot C, et al. **Axonal loss in multiple sclerosis lesions: magnetic resonance imaging insights into substrates of disability.** *Ann Neurol* 1999;46:747-754
4. van Buchem MA, McGowan JC, Kolson DL, Polansky M, Grossman RI. **Quantitative volumetric magnetization transfer analysis in multiple sclerosis: estimation of macroscopic and microscopic disease burden.** *Magn Reson Med* 1996;36:632-636
5. Tortorella C, Viti B, Bozzali M, et al. **A magnetization transfer histogram study of normal-appearing brain tissue in MS.** *Neurology* 2000;54:186-193
6. Barker GJ, Tofts PS, Gass A. **An interleaved sequence for accurate and reproducible clinical measurement of magnetization transfer ratio.** *Magn Reson Imaging* 1996;14:403-411
7. Balaban RS, Ceckler TL. **Magnetization transfer contrast in magnetic resonance imaging.** *Magn Reson Q* 1992;8:116-137
8. Studholme C, Hill DLG, Hawkes DJ. **Automated three-dimensional registration of magnetic resonance and positron emission tomography brain images by multiresolution optimization of voxel similarity measures.** *Med Phys* 1996;24:25-35
9. Rovaris M, Filippi M, Calori G, et al. **Intra-observer reproducibility in measuring new putative MR markers of demyelination and axonal loss in multiple sclerosis: a comparison with conventional T2-weighted images.** *J Neurol* 1997;244:266-270
10. Filippi M, Iannucci G, Tortorella C, et al. **Comparison of MS clinical phenotypes using conventional and magnetization transfer MRI.** *Neurology* 1999;52:588-594
11. Efron B, Tibshirani R. **Statistical data analysis in the computer age.** *Science* 1999;253:390-395
12. Sormani MP, Iannucci G, Rocca MA, et al. **Reproducibility of magnetization transfer ratio histogram-derived measures of the brain in healthy volunteers.** *AJNR Am J Neuroradiol* 2000;21:133-136
13. Filippi M, Horsfield MA, Campi A, Mammi S, Pereira C, Comi G. **Resolution-dependent estimates of lesion volumes in magnetic resonance imaging studies of the brain in multiple sclerosis.** *Ann Neurol* 1995;38:749-754